

Temporal Evolution in the Spectra of Gradual Solar Energetic Particle Events

Allan J. Tylka¹, Paul R. Boberg^{2,1}, Robert E. McGuire³,
Chee K. Ng^{4,5}, and Donald V. Reames⁴

¹*E.O. Hulburt Center for Space Research, Naval Research Laboratory*, ²*Consultant*

³*National Space Science Data Center, NASA Goddard Space Flight Center*

⁴*Laboratory for High Energy Astrophysics, NASA Goddard Space Flight Center*

⁵*Dept. of Astronomy, University of Maryland*

Abstract. We examine solar energetic particle (SEP) spectra in two very large “gradual” events (20 April 1998 and 25 August 1998), in which acceleration is caused by fast CME-driven shocks. By combining data from ACE/SIS, Wind/EPACT/LEMT, and IMP8/GME, we examine all major species from H to Fe, from ~ 2 MeV/nuc to the highest energies measured. These events last for several days, so we have divided the events into 8-hour intervals in order to study the evolution of the spectra. The spectra reveal significant departures from simple power laws. Of particular note is the behavior at high energies, where the spectra exhibit exponential rollovers. We demonstrate that the fitted e-folding energies reflect both ionic charge states and a complex but orderly temporal evolution. We speculate that this behavior may be related to evolving rigidity dependence in the near-shock diffusion coefficient, which is of potentially great importance for models of SEP acceleration and transport.

INTRODUCTION

In this paper, we focus on the two largest “gradual” SEP events seen so far in Solar Cycle 23: 20 April 1998, which had the largest fluence of >10 MeV/nuc particles; and 25 August 1998, which had the highest intensities of \sim MeV/nuc particles. Both of these events were caused by fast CME-driven shocks. CMEs and shocks certainly slow down [1] and otherwise evolve as they move through the changing interplanetary plasma conditions of the inner heliosphere. This evolution should be reflected in the SEP spectra. Thus, unlike nearly all previous SEP studies [e.g., 2, 3], we do not simply examine event-integrated spectra. Instead, we take advantage of the large geometry factors of Wind/EPACT/LEMT [4] and ACE/SIS [5] to investigate how the spectral characteristics evolve during the event. We combine these data with extensive H and He measurements from IMP-8/GME [6]. As we shall demonstrate, the H and He spectra provide a critical ‘calibration’ for understanding the spectra of heavier ions.

Ellison and Ramaty [7] have discussed shock-theory expectations for SEP spectra. The differential energy spectrum of ion species X should follow a power-law, modulated by an exponential,

$$F_X(E) = C_X \cdot (E^2 + 2ME)^{-\gamma} \cdot \exp(-E/E_{0X}) \quad (1)$$

where C_X is a normalization factor and $M = 938.3$ MeV/nuc. The spectral index γ is determined by the shock compression ratio and is the same for all species. The exponential rollover at high energies is caused by finite shock-lifetime and/or finite shock-size effects. Moreover, if the diffusion coefficient at the shock has the form $\kappa \sim \beta R^\alpha$ (β = particle speed, R = rigidity) with $\alpha = 1$, then the e-folding energy E_{0X} varies from species to species, with a value which is directly proportional to the ion’s charge-to-mass ratio, Q_x/A_x . Strictly speaking, equation (1) applies only at the shock. But we will nevertheless compare it to observed spectra, implicitly assuming that effects related to escape from the shock region and subsequent interplanetary transport are relatively small at sufficiently large rigidities.

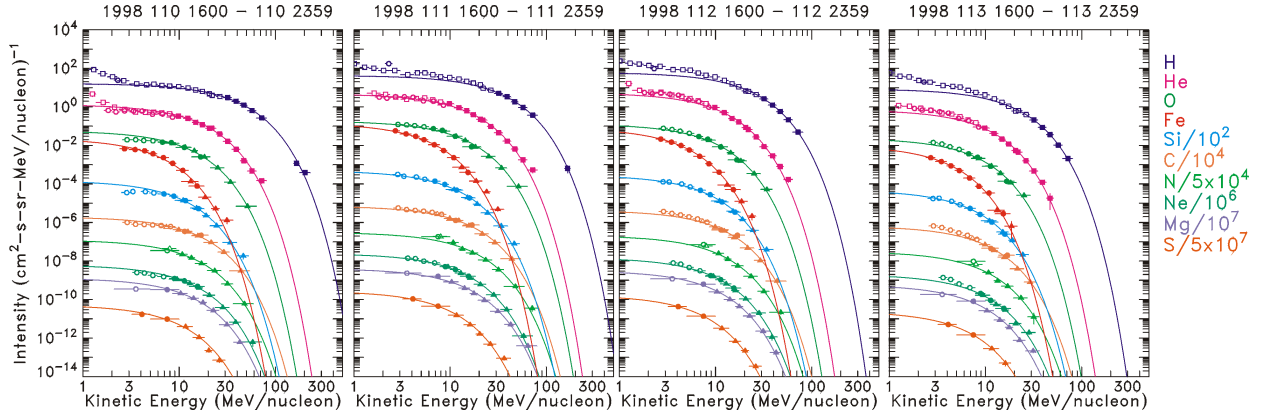


Figure 1. Examples of 8-hour-averaged spectra in the 20 April 1998 event. Each species is color-coded and shown in the same order from top to bottom as in the legend at the right. Note the scale factors used in plotting some elements. Data come from IMP-8/GME (■), Wind/EPACT/LEMT (●) and ACE/SIS (▲). Curves are exponential fits to the high-rigidity points. Open symbols denote low-rigidity points which were not used in the fits. Datapoints consistent with residual Galactic and/or anomalous cosmic-ray background are not shown.

20 APRIL 1998 EVENT

This SEP event was caused by a fast (~1600 km/s) western-limb CME which was first detected by SoHO/LASCO at 10:07 UT on 20 April 1998. The associated flare (~W87) was well removed from the footpoint of the Sun-Earth field line, and flare and CME activity were low in the preceding ~2 weeks. Thus, this event has provided an unusually “clean” baseline for studying gradual events. The event shows strong systematic variation in elemental composition [8] due to rigidity-dependent transport through proton-amplified Alfvén waves [9, 10].

Figure 1 shows a sample of the thirteen 8-hour averaged particle spectra starting at 16 UT on 20 April 1998 (DOY 110), ~6 hours after onset so as to avoid initial dispersion effects. Non-SEP backgrounds (as estimated from solar-quiet periods [11]) have been subtracted. In addition, slight adjustments have been made for normalization discrepancies (typically ~10-20%) among the instruments. These adjustments have been applied “globally” to all measurements in each 8-hour interval, so as to preserve the spectral shapes reported by each instrument.

Eight hours is long compared to Sun-Earth transit times at these energies, so residual velocity dispersion effects should be small. At low energies, these spectra are very flat, with spectral index $\gamma \sim 0$. This value is inconsistent with any physical shock compression ratio. In fact, this flattening is another reflection of

rigidity-dependent escape from the shock region [9]. When these spectra are plotted vs. rigidity [8], assuming typical charge states, the plateaus extend to ~230 MV. Thus, in order to minimize the impact of such transport effects in this analysis, the exponential fits in Figure 1 have used only datapoints corresponding to rigidity >230 MV.

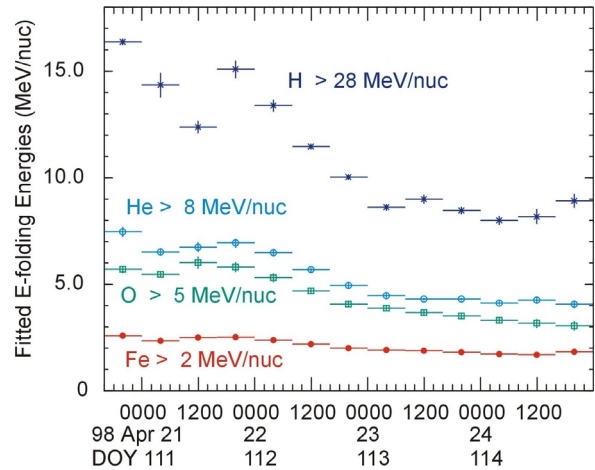


FIGURE 2. E-folding energies E_0 vs. time, from exponential fits of high-energy H, He, O, and Fe in Figure 1.

The steepness of the Fe rollover relative to that of other heavy ions is particularly striking. As seen in Figure 1, exponentials generally provide acceptable fits to the high-rigidity parts of the spectra throughout this event. Figure 2 shows temporal evolution of the

fitted e-folding energies (E_0) for some species (H, He, O, and Fe). E_0 values decline more or less smoothly during the first ~ 3 days of the event¹. However, starting shortly before shock arrival at ~ 17 UT on DOY 113, E_0 values become roughly constant. This behavior is consistent with onset of the invariant spectrum region [12, 13].

The fitted E_0 values in Figure 2 are roughly proportional to Q/A , as suggested by Ellison & Ramaty [7] for $\kappa \sim \beta R$. But careful examination shows that $E_{0\text{He}}/E_{0\text{H}}$ differs by a small but significant amount from 0.5 early in the event. As a slightly more complicated alternative, we therefore consider e-folding energies proportional to a *power* of Q/A , i.e.,

$$E_{0x} = E_{0\text{H}} (Q_x/A_x)^\delta \quad (2)$$

Figure 3 shows the values of δ , as determined from the He E_0 values, assuming that the He ions are fully stripped. These δ values are generally, but not always, close to unity.

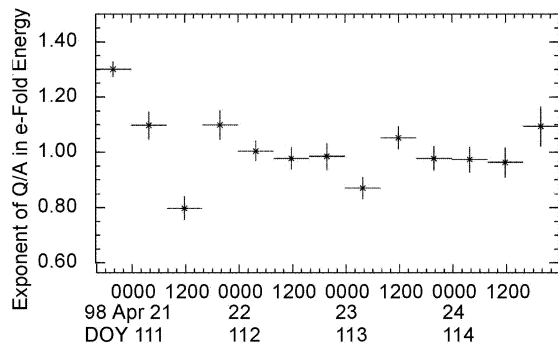


FIGURE 3. Value of the exponent δ in equation (2), as determined from H and He.

We have thus used the proton and alpha spectra to “calibrate” the Q/A dependence of E_0 in this event. We now employ equation (2), along with the $E_{0\text{H}}$ values in Figure 2 and the δ values in Figure 3, to infer charge states for all the other species in each time interval. Figure 4 shows these results. There is little time dependence in these charge states. ACE/SEPICA also reports virtually no time dependence in their directly measured charge states at ~ 0.2 - 1.0 MeV/nuc in this event [14].

Table 1 compares the mean charge states (from averaging over all time intervals) with those reported

¹ The exception is a slight increase in E_0 values between Periods 3 and 4. This increase appears to be associated with abrupt changes in particle intensities and large fluctuations in magnetic field directions, perhaps indicating a change in our connection to the CME-driven shockfront.

by ACE/SEPICA for this event [14]. The values² agree remarkably well, except for Mg. In fact, all of the charge states in Table 1 are typical of the solar wind and consistent with a single source plasma temperature of ~ 1.5 MK, except for the ACE/SEPICA Mg result, which is low by ~ 1 charge unit [14].

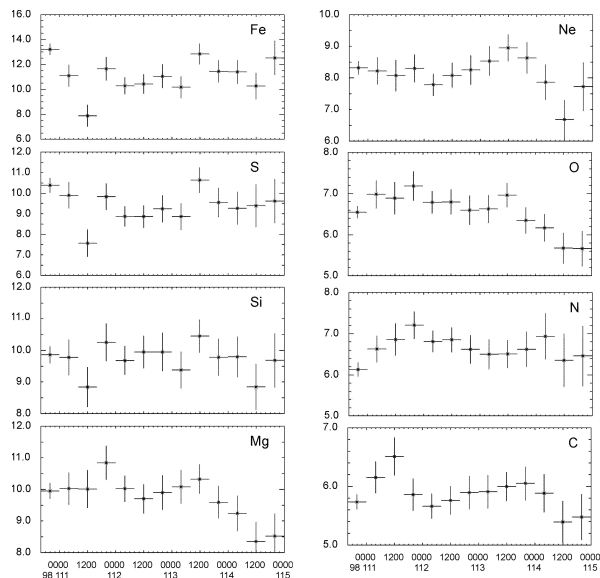


Figure 4. Inferred charge states vs. time in the 20 April 1998 event.

TABLE 1. Mean SEP Charge States: 20-25 April 1998

Element	ACE/SEPICA $\sim 0.2 - 1.0$ MeV/nuc	This Analysis $\sim 2 - 60$ MeV/nuc
C	5.68 ± 0.17	5.85 ± 0.17
N	--	6.6 ± 0.1
O	6.92 ± 0.17	6.59 ± 0.08
Ne	8.27 ± 0.23	8.20 ± 0.11
Mg	8.96 ± 0.26	9.84 ± 0.13
Si	9.67 ± 0.29	9.78 ± 0.14
S	--	9.5 ± 0.2
Fe	11.68 ± 0.29	11.4 ± 0.2

The internal consistency of these charge state determinations suggests that fitted E_0 values are indeed meaningful quantities. But it is important to understand *why* these spectral fits reflect the charge states so well in this particular event. For example, we

² Table 1 shows only formal errors from the fitting procedures and error propagation. In order to assess potential *systematic* errors in this study, we repeated the charge-state analysis using the full equation (1) form (not just an exponential) and all datapoints above 2.4 MeV/nuc (not just those at high rigidity). This yielded slightly different E_0 values, but none of the average inferred charge states changed by more than 6%.

would not expect good fits to the Fe spectra if the Fe ions actually arose from a broad distribution of charge states. But according to ACE/SEPICA, this event has one of the narrowest SEP Fe charge distributions observed so far [M. Popecki, private communication], perhaps because of the relative dearth of preceding solar activity [15].

Similarly, why is there apparently so little energy dependence in the charge states of this event? There are now several examples of events in which the ionic charge states have significant energy dependence [16, 17, 18]. Such energy dependence would also foil our charge state determinations. But Reames et al. [19] recently suggested that this energy dependence arises when acceleration begins in high-density regions low in the corona, at altitudes below 0.2 Rs. In this particular event, however, electron onset times in the Wind/3DP experiment (S. Krucker, private communication) indicate that energetic particles were first deposited on the Sun-Earth field line at 10:19 UT *at the Sun*. SoHO/LASCO shows that the leading edge of the CME was already ~ 4.4 Rs above the solar surface at this time (O.C. St. Cyr, private communication). Thus, in this event, it is likely that we saw *here at Earth* only particles which had been accelerated in low-density regions. Hence, no further stripping – and no strongly energy-dependent charge states – should be expected in this event.

25 AUGUST 1998 EVENT

The 25 August (DOY 237) 1998 SEP event offers an instructive comparison to the 20 April 1998 event

[8]. This was a central meridian event, associated with an X1.0 flare at N35E09 at 21:50 UT on DOY 236. A strong IP shock arrived at Earth ~ 34 hours later, corresponding to a mean transit speed of ~ 1200 km/s. SoHO/LASCO observations are unavailable, but this event was presumably associated with a fast halo CME. As in the 20 April 1998 event, the footpoint of the Sun-Earth field line was far removed from the flare site; it is thus unlikely that we saw flare-accelerated particles. But, whereas the 20 April 1998 event only showed us particles accelerated in the relatively weak shock at the far-eastern flank of the CME, in this case we observe particles coming from strong parts of the shock for most of the event. Also, unlike the relatively quiet conditions that preceded the April event, two smaller SEP events occurred in the week preceding this event.

Figure 5 shows a sample of 8-hour averaged particle spectra in this event. Exponential rollovers are difficult to detect early in the event, presumably because they occur at energies above the range of these data. The protons in the first panel, for example, are consistent with a power law spectrum from ~ 5 to 500 MeV. Later in the event, the exponential rollovers become apparent. Curves in Figure 5 are fits to equation (1), with each species having its own E_{0X} but constrained to keep the same power law index γ as protons. Flattening relative to the power law is seen in this event too, but only at energies below ~ 3 MeV/nuc and mostly early in the event.

The Fe spectrum is particularly noteworthy in Figure 5. The measured Fe intensities are well above GCR background levels. But in the first panel, the Fe spectrum is complicated and cannot be fit by the

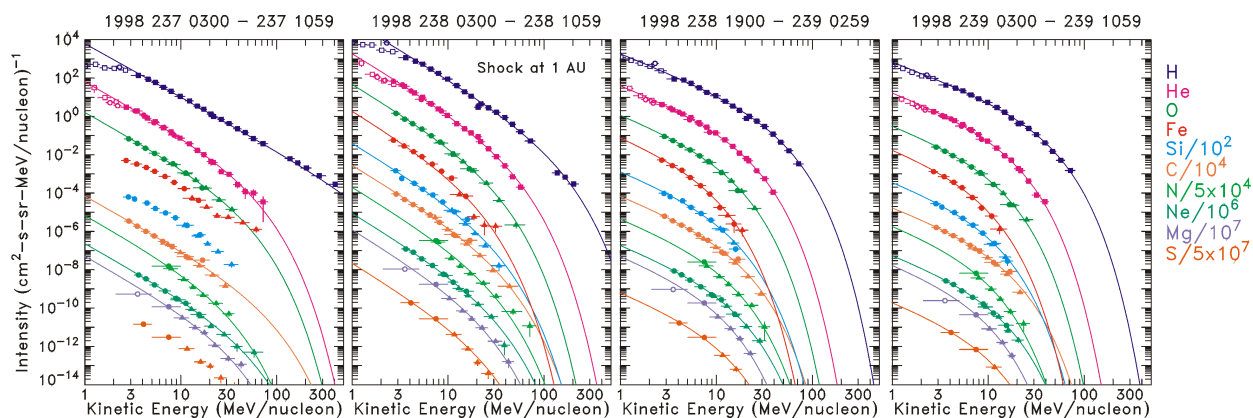


Figure 5. Examples of 8-hour-averaged spectra in the 25 August 1998 event. Symbols are as in Figure 1. Curves are fits to equation (1), using all datapoints above 2.4 MeV/nuc. Open symbols denote low-energy points that were not used in the fits. No satisfactory fits were found for Fe, S, and Si in the first panel. The shock arrived at 1 AU at the middle of the time period covered by the second panel.

simple functional form of equation (1). Similar problems appear for S and Si. Only later in the event does this form work reasonably well for these species. When integrated over the entire event duration, this event is “Fe poor” at ACE/SIS energies. But in the first time interval, the Fe/O ratio increases with energy and approaches unity (or perhaps even to exceeds it) at the highest energies. Other events have shown this behavior in event-integrated spectra [3].

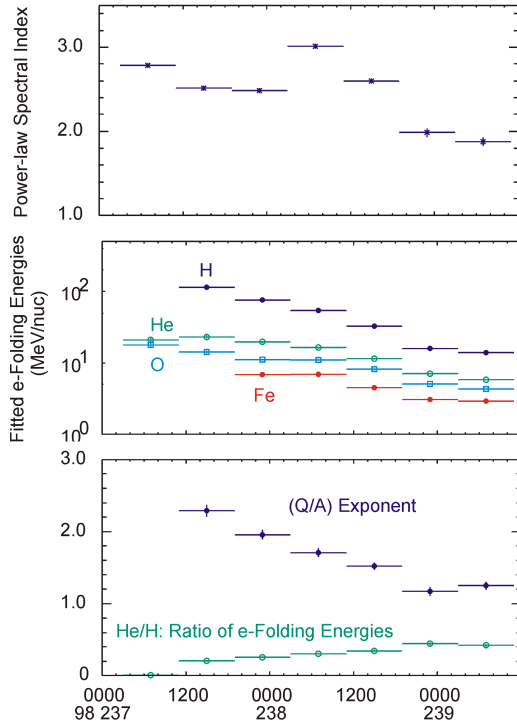


FIGURE 6. Evolution of fit parameters in the 25 August 1998 event. (a) top: power-law spectral index γ ; (b) middle: E_0 for H, He, O, and Fe; (c) bottom: ratio $E_{0\text{He}}$ to $E_{0\text{H}}$, and exponent δ for equation (2), as determined from H and He.

Figure 6a shows the power law spectral indices, as determined from the protons. Shock passage occurs in the middle of the fourth interval. The spectral indices are significantly smaller both before and after shock passage. This suggests that the apparent temporal evolution in the spectral index may be more related to transport effects, rather than changes in the compression ratio. Such transport effects are likely to be rigidity dependent. Our procedure of constraining all species to have the same γ as protons is therefore probably not strictly correct, even though it appears to work reasonably well.

Figure 6b shows the fitted E_0 energies for H, He, O, and Fe, except for H in the first time interval (where $E_{0\text{H}}$ cannot be determined since no rollover is

observed below 500 MeV) and Fe in the first two intervals (where fits to equation (1) fail). *The E_0 energies in this event are much larger and evolve more rapidly than in the April event.* Only late in the event, in the post-shock invariant spectrum region, do these E_0 values become similar to those of the April event.

Figure 6c plots the ratio of the fitted E_0 energies for H and He. This ratio does not attain ~ 0.5 until late in the event. The direct proportionality $E_0 \sim Q/A$ thus does not apply throughout most of this event. Figure 6c also shows the values of exponent δ for equation (2), derived from the fitted H and He E_0 values. Initially, $\delta \sim 2.4$ (and perhaps even larger, since we cannot determine $E_{0\text{H}}$ in the first time interval) and evolves smoothly towards unity. *Again, this behavior is quite different from the relatively weak Q/A dependence shown in Figure 3 for the April event.*

Finally, Figure 7 shows the ionic charge states we deduce by applying equation (2) and the parameters from Figure 6 to other species. No charge states are shown for the first time interval, where $E_{0\text{H}}$ could not be determined; nor for Fe in the second interval, where the Fe spectrum was inconsistent with equation (1). In this event, the inferred charge states are not consistent with a single plasma temperature. No ACE/SEPICA measurements are available for this event. However, these inferred charge states are similar to previous measurements of gradual events. In particular, the mean Fe charge state here agrees well with the result reported by SAMPEX/MAST in the Oct-Nov. 1992 event at ~ 15 -70 MeV/nuc [20]. The higher Fe charge state here (compared to the April event) may also be indicative of a source population comprising a mixture of solar-wind and coronal [21] and/or remnant flare-accelerated suprathermals [15].

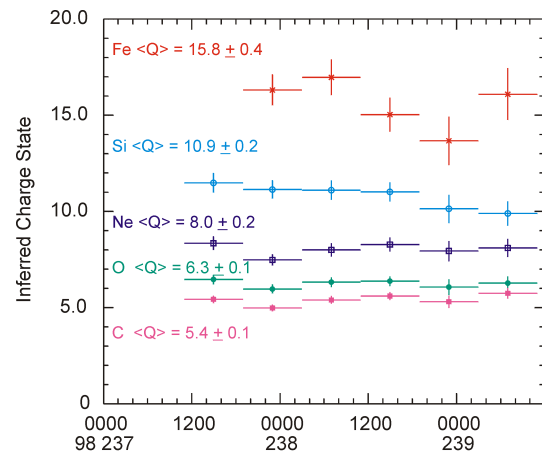


FIGURE 7. Inferred charge states vs. time in the 25 August 1998 event.

DISCUSSION AND CONCLUSIONS

The two events considered here show a complex but orderly pattern in the temporal evolution of SEP spectral shapes that was inaccessible to earlier instruments. The striking cogency of the charge state determinations suggests that the fitted e-folding energies do indeed contain fundamental information about the acceleration process. According to Ellison & Ramaty [7], we should expect $E_{0x} \sim Q_x/A_x$ when the near-shock diffusion coefficient is proportional to the first power of rigidity. It is therefore tempting to think that the stronger Q/A dependence in e-folding energies of the August event reflects even stronger rigidity dependence in the near-shock scattering. But what drives the temporal evolution of the scattering during the event? And why are scattering conditions so different in these two events? Indeed, there are other events in the historical record in which the spectral rollovers occur at much higher energies. For example, in the 29 September 1989 event, Lovell et al. [22] showed that the proton spectrum had $E_0 \sim 1$ GeV!

We now know that in very large SEP events, escape from the shock region and subsequent interplanetary transport is governed by Alfvén waves amplified by the streaming energetic protons themselves [8, 9, 10]. These same waves presumably also have significant impact on acceleration efficiency, through the increase in cross-shock scattering that they cause. Moreover, the spectrum of these proton-amplified waves is highly dynamic. Thus, it is also tempting to think that these waves play a key role in the observed spectral evolution.

The behavior of the Fe spectrum early in the August event is particularly puzzling. In part, this behavior may reflect energy-dependent charge states and/or a broad distribution of Fe charge states. But it is hard to see, at least in the context of the modeling discussed here, how the Fe spectrum could ever extend beyond the oxygen spectrum, no matter what the Fe charge state may be. A critical assumption in arriving at this relatively simple Q/A-dependence in the e-folding energies is that the near-shock scattering can always be adequately characterized as a *single, decreasing* power-law function in rigidity, applicable over a wide range of rigidities. However, proton-amplified waves generate scattering with complex rigidity dependence. Thus, these waves may also be important in understanding these complex spectra.

In summary, high-energy SEP spectra provide us with a kind of ‘remote sensing’, in which exponential rollovers probe scattering conditions in the shock region, even when the shock is still far from Earth.

However, it should be noted that in many events, these rollovers cannot be adequately defined with the limited energy range of current instruments. This is especially true for protons and alphas. Future SEP experiments should extend spectral measurements to \sim GeV/nuc energies. In addition, as we have shown here, high-energy charge states critically test our understanding of these spectra. Thus, new experiments should also provide a follow-on to SAMPEX [17,20] and LDEF [23], with sufficient collecting power to track temporal evolution in charge states at \sim 10-100 MeV/nuc.

ACKNOWLEDGMENTS

We thank B. Klecker, S. Krucker, M. Popecki, and O.C. St. Cyr for helpful discussions. AJT and PRB gratefully acknowledge support by the ACE Guest Investigator Program, under NASA DPR#W-19501.

REFERENCES

1. Sheeley, N.R. Jr. et al., *JGR* **104**, 24739-24768 (1999).
2. Mazur, J.E. et al., *Ap.J.* **401**, 398-410 (1992).
3. Tylka, A.J. and Dietrich, W.F., *Radiat. Meas.* **30**, 345-359 (1999).
4. von Rosenvinge, T.T. et al., *Sp.Sci.Rev.* **71**, 155-206 (1995).
5. Stone, E.C. et al., *Sp.Sci.Rev.* **86**, 357-408 (1998).
6. McGuire, R.E. et al., *Ap.J.* **301**, 938-961 (1986).
7. Ellison, D. and Ramaty, R., *Ap.J.* **298**, 400-408 (1985).
8. Tylka, A.J. et al., *GRL* **26**, 2141-2144 (1999).
9. Ng, C.K. et al., *GRL* **26**, 2145-2148 (1999).
10. Lee, M.A., *JGR* **88**, 6109-6119 (1983).
11. Leske, R.A. et al., *Proc. 26th ICRC* **7**, 539-542 (1999).
12. Reames, D.V. et al., *Ap.J.* **491**, 414-420 (1997).
13. Kahler, S.W. et al., *Proc. 26th ICRC* **6**, 26-29 (1999).
14. Klecker, B. et al., *Proc. 26th ICRC* **6**, 83-86 (1999).
15. Mason, G.M., et al., *Ap.J. Lett.* **525**, L133-L136 (1999).
16. Oetliker, M. et al., *Ap.J.* **477**, 495-501 (1997).
17. Mazur, J.E. et al., *GRL* **26**, 173-176 (1999).
18. Moebius, E. et al., *GRL* **26**, 145-148 (1999).
19. Reames, D.V. et al., *GRL* **26**, 3585-3588 (1999).
20. Leske, R.A. et al., *Ap.J. Lett.* **452**, L149-L152 (1995).
21. Boberg, P.R. et al., *Ap.J. Lett.* **471**, L65-L68 (1996).
22. Lovell, J.L. et al., *JGR* **103**, 23733-23742 (1998).
23. Tylka, A.J. et al., *Ap.J. Lett.* **444**, L109-L113 (1995).